The Bioscan AN INTERNATIONAL QUARTERLY JOURNAL OF LIFE SCIENCES 20(4): 1082-1096,2025 www.thebioscan.com

Bio-Synthesis and Characterization of CuO and Ag doped CuO nanoparticles using Cissampelos Pareira and their Anti-cancer applications

H. R. Uma[1] and Jessica Fernando[2]

1. Research Scholar (Register No: 20113112032013) Department of Chemistry, V. O. Chidambaram College, Thoothukudi - 628 008, Affiliated to Manonmaniam Sundaranar University, Abishekapatti - 627 012, Tamil Nadu, India, Tamil Nadu, India

Email: umahrchem@gmail.com

2. Associate Professor, Department of Chemistry, V. O. Chidambaram College, Thoothukudi - 628 008, Affiliated to Manonmaniam Sundaranar University, Abishekapatti - 627 012, Tamil Nadu, India, Tamil Nadu, India

Email: jessivoc@yahoo.com

DOI: 10.63001/tbs.2025.v20.i04.pp1082-1096

KEYWORDS

Green Synthesis, Nanoparticles, Cissampelos pareira leaves, Anticancer activity, Cell viability

Received on: 30-10-2025

Accepted on: 05-11-2025

Published on: 09-11-2025

Abstract

This research aimed to evaluate the antitumor efficacy of these nanoparticles against AGS cancer cells. Pure CuO and Ag-doped CuO nanoparticles were produced and studied using X-ray diffraction (XRD), energy-dispersive spectroscopy (EDS), transmission electron microscopy (TEM), X-ray photoelectron spectroscopy (XPS), and UV-visible spectroscopy. The anti-cancer efficacy of the biogenically produced nanoparticles was assessed against AGS cancer cells. The produced Pure CuO and Ag-doped CuO nanoparticles and plant extract characterised displayed a lethal effect on AGS cancer cells. In addition to these exciting discoveries, the materials deactivate against an AGS cell line by an MTT trial, which revealed the superiority of the doped as compared to the native nanoparticles. As a consequence, these findings revealed that the produced biogenic nanoparticles are suitable candidates for cancer therapy in the biomedical area as an anticancer agent.

1. Introduction

Metal and metal oxide nanoparticles are receiving considerable attention in recent times owing to their improved and modifiable surface morphology, physic-chemical characteristics, extremely small size and huge surface area [1]. Most of the nanoparticle synthesis techniques employ physical, biological and chemical methods, which are expensive and release harmful chemicals resulting into severe environmental pollution [2]. Hence it is required to develop non-toxic and cost effective methods to synthesize metal oxide nanoparticles employing eco-friendly techniques [3,4]. Green synthesis methods are practiced by researchers to produce nanoparticles from natural plant extracts which are rich in phytochemicals such as alkaloids, poly phenols, proteins, vitamins, flavonoids etc, which act as both reducing and capping agents [5]. The factors affecting the biosynthesis of nanoparticles are temperature, time, concentration, pH, pressure and the nature of solvents [6]. By careful control and documentation of capping agents and appropriate functional groups on the surface of nanoparticles, the particle size, shape, agglomeration, surface energy, grain development, dispersion and electrostatic forces can be regulated [7]. Cissampelos Pareira of the family Menispermaceae is commonly known as Patha in Ayurveda and have been used for the treatment of fever, urinary problems and skin infections [8]. Various alkaloids and different pharmacological activities of these plants have been reported. C. Pareira extracts were tested for Antipyretic activity, Chemomodulatory influence of Hirsuta on Gastric cancer and antioxidant system in experimental animal, anti-infammatory activity, Immunomodulatory activity, antifertility activity, antinociceptic antiarthritic activity, antibacterial activity, antimalarial activity, diuretic activity, hypoglycemic activity and anticonvulsant activity [9]. Among various nanoparticles, transition metal oxide nanoparticles have wide application in various fields viz. chemistry, physics, material science, biotechnology, environmental technology etc [10]. CuO nanoparticles receive lot of attention for their versatile properties and potential use as gas sensors, solar cells, lithium ion batteries, heterogeneous catalysts and antibacterial agents. Besides CuO nanoparticles are stable, robust and have a longer shelf life compared to oraganic, antimicrobial agents [4,11–13]. It is why the present study stands significant as it deals

with green synthesis of CuO nanoparticles and Ag doped CuO nanoparticles employing C.Pareira leaf extract and testing their efficient as anticanceral agents against AGS human gastric adenocarcinoma cells.

2. Materials and methods

2.1 Materials

Copper (II) nitrate, silver nitrate ($AgNO_3$) and Sodium hydroxide (NaOH) were the chemical reagents that were utilized in this study. Both of these reagents were obtained from SRL Chemicals and had a purity level of 99%. Additionally, all of the reagents that were utilized were of analytical grade and were utilized without any additional purification. Every single one of the aqueous solutions was made with water that had been double-distilled.

2.2 Preparation of leaf Extract

The leaves of Cissampelos Pareira were collected, given a thorough cleaning with tap water, followed by repeated washings with double-distilled (DD) water, and then dried. Before boiling at 80°C, 30g of leaves were combined with 150 ml of DD water. The procedure resulted in the formation of a solution that was yellow in color. After that, the extract that had been prepared was allowed to cool at ambient temperature, and then, as a last step, it was filtered using Whatman filter paper and placed in a refrigerator for later use.

2.3 Synthesis of pure copper oxide nanoparticles

5g of copper nitrate were dissolved in 50 ml of water that had been double-distilled. After that, 10 ml of leaf extract are added to the solution while it is being stirred continuously. After that, NaOH is added to the solution that will be used to alter the pH to 9. For a period of 2h, the solution was maintained on the magnetic stirrer. A precipitate was produced as a result. It took 24h of undisturbed time for the precipitate to settle in the solution. For the purpose of further characterization, the precipitate that was obtained is filtered and washed with DD water and ethanol concurrently. After that, it is dried and muffled at a temperature of 500°C for 2h.

2.4 Synthesis of silver doped copper oxide nanoparticles

50 ml of DD water were used to dissolve 5g of copper nitrate 0.5g of $AgNO_3$. After that, 10 ml of leaf extract are added to the solution while it is being stirred continuously. After that, NaOH is added to the solution that will be used to alter the pH to 9. For a period of 2h, the solution was maintained on the magnetic stirrer. A precipitate was produced as a result. It took 24h of undisturbed time for the precipitate to

settle in the solution. For the purpose of further characterization, the precipitate that was obtained is filtered and washed with DD water and ethanol concurrently. After that, it is dried and muffled at a temperature of 500°C for 2h.

2.5 Characterization section

The X-ray diffraction (XRD) technique specifically the ARL EQUINOX 3000, with wavelength of 1.5406 Å, a voltage of 40 kV, and a current of 30 mA, was utilized to look into the crystal structure, phase determination, and average crystallite size of the samples that wer manufactured. In order to create the micrograph of the nanoparticles, a transmission electron microscope (TEM) with a JEOL-JEM-2100F and an accelerating voltage of 200 kV was utilized For the purpose of analyzing Zn 2p, O 1s, and Ag 3d peaks, the X-ray Photoelectron Spectroscopic (XPS) measurement was carried out by utilizing a Photoelectron spectrometer (Thermo Fisher Scientific, USA)that was outfitted with a high-performance 0–5 keV Ar + ion gun as well as optional 10 and 20 kV C60 ion guns. In order to evaluate the samples, an ultraviolet absorbance spectrophotometer (Perkin Elmer LAMBDA – 35) was used to analyse the visible and ultraviolet spectra of the samples that were synthesized. The experiment was carried out at room temperature. At a temperature of room temperature, the PL spectra of the materials were acquired with the use of a Cary Eclipse Photoluminescence Spectrophotometer.

2.5.Anticancer activity

The human stomach adenocarcinoma cell line, often known as AGS, was obtained from the National Cancer Center in Pune, India. Two days later, the cells were subcultured in DMEM/F12 media that was supplemented with 10% FBS and 1% antibiotic-antimycotic solution. The cells were then placed in a CO_2 incubator at a temperature of 370°C with a CO_2 atmosphere of 5% carbon dioxide and 18–20% oxygen. For the purpose of this investigation, the passage number was determined to be 37 AGS cells.

First, on a 96-well plate, place a 200 µl suspension of cells at the required cell density of 10,000 cells per well. Then, allow the cells to mature for approximately 24h. At the appropriate concentrations, which have been diluted over the entire medium, add the test substances that have been indicated. It is recommended that the plate be incubated for twenty-four hours at 37°C with 5% CO_2 in the air. After the incubation period has ended, remove the plates from the incubator, throw away any medium that has been unused, and then add MTT reagent until the final concentration reaches 0.5 mg/ml of the total volume. If you want to prevent the plate from

being exposed to light, you should cover it in aluminum foil. Reintroduce the plates to the incubator, and then allow them to remain there for a period of three hours. Incubation times vary from cell line to cell line, depending on the type of cell. When doing comparisons within the context of a single experiment, it is important to ensure that the incubation duration remains unchanged. The MTT should be removed.

$$Cell\ viability\ (\%) = \frac{OD\ sample\ mean}{OD\ control\ mean} \times 100\%$$

3. Results and Discussion

3.1 XRD Analysis

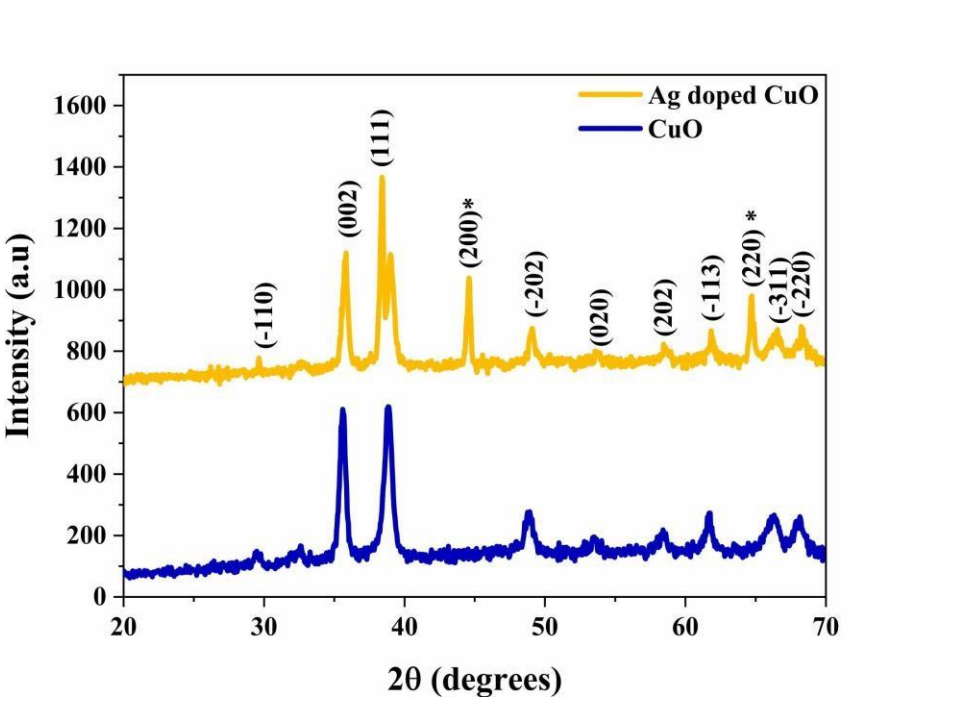

Figure 1 XRD pattern of CuO and Ag doped CuO nanoparticles

Figure 1 shows the XRD pattern of CuO and Ag doped CuO nanoparticles. The XRD pattern of the CuO exhibits diffraction peaks at 2θ = 29.58º, 35.74º, 38.48º, 49.16º, 53.78º, 58.48º, 61.81º, 66.60º and 68.31º which could be indexed to the planes (-110), (002), (111), (-202), (020), (202), (-113), (-311) and (-220) respectively of monoclinic CuO (see JCPDS card no: 45-0937) with strong crystallinity. In addition to these, Ag doped CuO samples exhibit two additional peaks centered at 2θ = 44.64º and 64.72º corresponding to (200) and (220) (JCPDS card no: 65-2871) and are marked with(in figure 1). Using the Debye-Scherrer formula, the

average crystallite size of the samples was calculated. The formula is as follows:

$$D = \frac{0.9\lambda}{\beta \cos\theta} \text{----------(1)}$$

Where 'D' stands for average grain size, 'λ' is the wavelength of Cu Kα radiation (λ=1.5405), 'θ' is the diffraction angle (°), and 'β' is the full width at half maximum (FWHM) for the diffraction peak under investigation (in radians). Using Debye-Scherrer's equation, the crystallite size of CuO powder was determined to be just about 29.12 nm and that of Ag doped CuO sample was obtained to be 21.01 nm.

3.2 TEM analysis

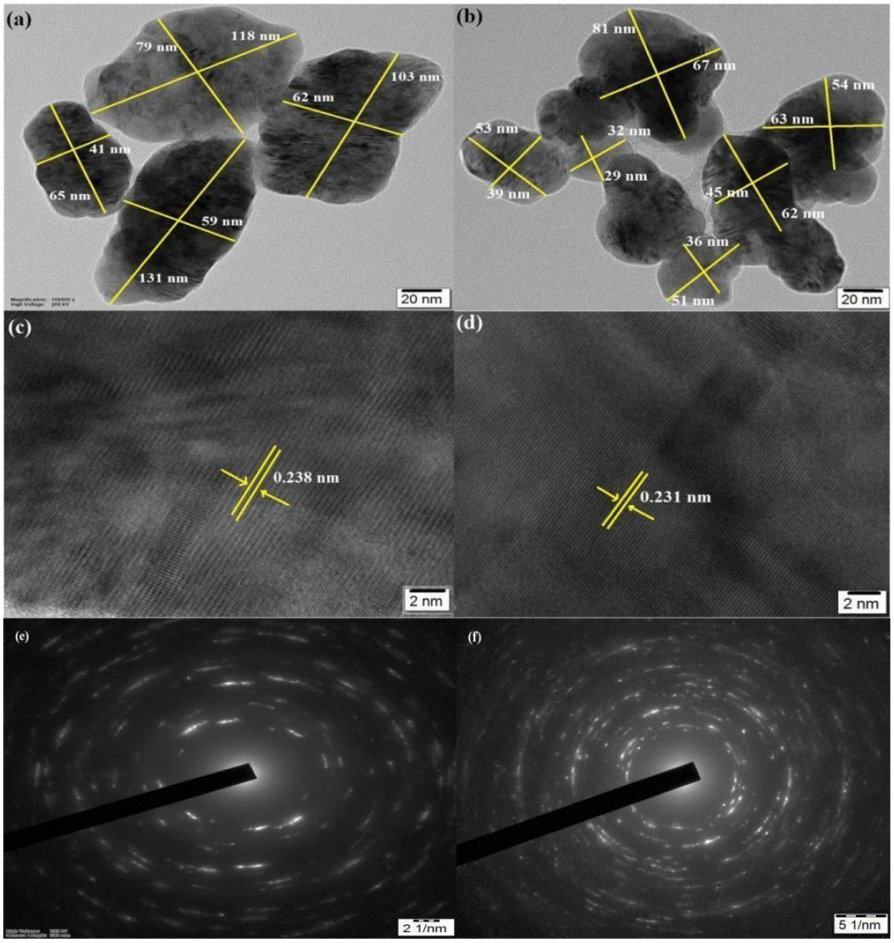

Fig. 2 (a and b) TEM image, (c and d) HRTEM image and SAED (e and f) of pure CuO and Ag doped CuO nanoparticles

As synthesised nanopowders were analysed by Transmission Electron Microscopy (TEM) and presented in Fig. 2 (a and b). The CuO and Ag doped CuO nanoparticles appeared to be

irregular and spherical shape. An average length and width of the pure CuO nanoparticles are determined to be 104.25 nm and 60.26 nm respectively. An average length and width of the Ag doped CuO nanoparticles are determined to be 56.11 nm and 44.73 nm respectively. Higher magnification analysis (HRTEM) showed a lattice planar spacing of 0.238 nm for pure CuO and 0.231 nm for Ag doped CuO nanoparticles, which was in agreement with literature value for the (111) plane (Fig. 2 (c and d) of 0.22 nm [14]. Fig. 2 (c and f) shows the SAED pattern of CuO and Ag doped CuO nanoparticles having diffraction rings with discrete diffraction spots, good agreement with the observed XRD results, which prove the monoclinic structure of CuO nanoparticles.

3.3 EDS spectral analysis

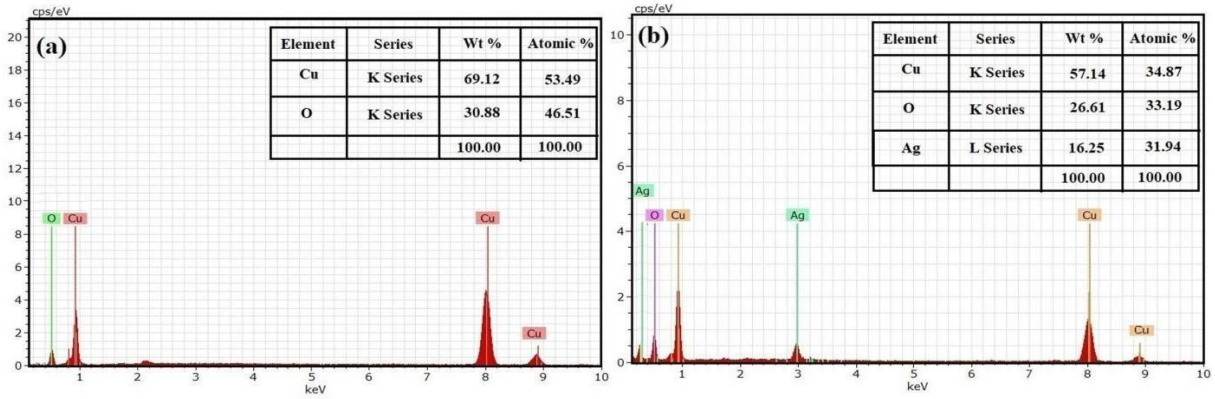

Figure 3 shows the EDS spectrum of pure CuO and Ag doped CuO.

From the EDS spectrum of CuO (figure 3(a)), the composition of copper (Cu) and oxygen (O) peaks approves the purity of CuO nanoparticles. Inset of the figure 3 (a), chemical composition (wt %) of Cu and O are found to be 69.12 % and 30.88 wt%, respectively. Moreover, the atomic percentages (%) are obtained at 53.49 % and 46.51 % for Cu and O, respectively. From the figure 3 (b), the existence of silver (Ag) peak in Ag doped CuO nanoparticles contributes to the doping of Ag in the CuO matrix. In the inset of figure 3 (b), chemical composition (wt %) of Cu, O and Ag are found to be 57.14 %, 26.61 % and 16.25 wt%, respectively. Moreover, the atomic percentages (%) are obtained at 34.87 %, 33.19 % and 31.94 % for Cu, O and Ag, respectively

3.3 XPS Analysis

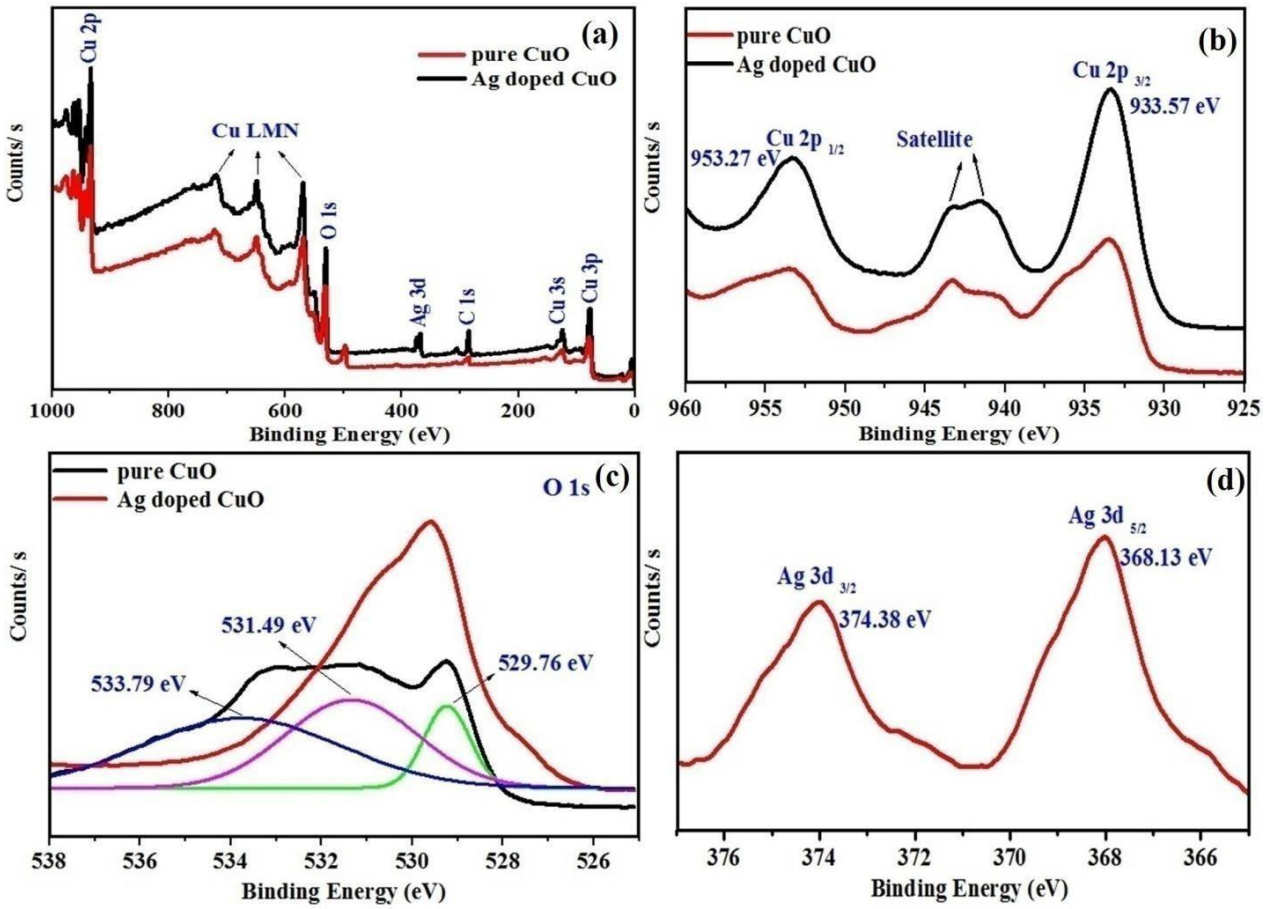

Figure 4(a) XPS survey spectrum of CuO and Ag doped CuO nanoparticles (b) Cu 2p region in CuO and Ag doped CuO nanoparticles (c) O 1s region in CuO and Ag doped CuO nanoparticles (d) Ag 3d region in Ag doped CuO nanoparticles

The survey spectrum of the prepared samples was shown in figure 4a. The CuO survey spectrum showed emission lines for Cu 2p, Cu 3s, Cu 3p, O 1s and auger peaks for Cu LMN. The Ag doped CuO survey spectrum additionally exhibited emission lines for Ag 3d, confirming the formation of Ag doped CuO nanoparticles. The high resolution XPS spectra provided insight into the chemical states of the elements. For Cu, the Cu 2p region showed peaks corresponding to Cu $2p_{3/2}$ and Cu $2p_{1/2}$ (Fig. 4b), confirming the presence of Cu^{2+} in both CuO and Ag doped CuO samples. The Cu 2p region showed peaks at 933.57 eV and 953.27 eV respectively for $2p_{3/2}$ and Cu $2p_{1/2}$ respectively. For O 1s region could be deconvoluted into two or three symmetric peaks, depending on the sample, with binding energies around 529, 531 and 533 eV (Fig. 4c). The Ag 3d peaks (Fig. 4d) were observed at binding energies around 368 eV and 374 eV for Ag doped CuO sample, corresponding to Ag $3d_{5/2}$ and Ag $3d_{3/2}$.

3.4 Photoluminescence

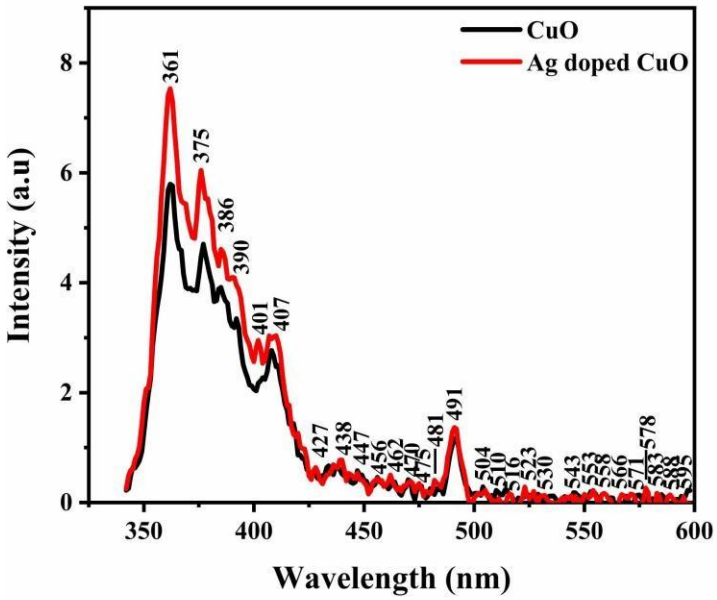

Figure 5 Photoluminescence spectra of CuO and Ag doped CuO nanoparticles

The as-synthesized nanocrystalline pure CuO and Ag doped CuO nanoparticles' room temperature photoluminescence spectra are displayed in the Fig. 5. The PL spectrum of the prepared samples shows several peaks at 361, 375, 386, 390, 401, 407, 427, 438, 447, 456, 462, 470, 475, 481, 491, 504, 510, 516, 523, 530, 543, 553, 558, 566, 571, 578, 583, 588, 595 nm. The visible emission is generally thought to be related to band gap defects such as O vacancies and Cu interstitials that form during particle growth [15]. The results obtained indicate that the near band edge (NBE) emission from the SnO_2 nanostructure is responsible for the peaks at 375, 386 and 390 nm [16], while the UV emission at 361 nm is ascribed to both radiative recombination of free exciton conduction band to acceptors and neutral donor bound excitons [16]. several luminous centres, such as defect energy levels resulting from oxygen vacancies and tin interstitials, as well as dangling bonds into nanocrystals, may be responsible for these emissions [17]. The most prevalent oxygen vacancy-related defects are V_o^0, V_o^+, and V_o^{++}. These

defects trap electrons from the valence band and have the potential to function as luminous centres inside the band gap [18]. Because of the creation of doubly ionised oxygen vacancies, there are emissions in the broad visible range between 400 and 500 nm. A hole is left in the valence band when an electron is stimulated from the valence band to the conduction band by the exposure of light. When an electron in the deep trap (V_o^+) recombines with this active hole, a V_o^{++} centre is created. This V_o^{++} centre then recombines with a conduction band electron to produce visible emission [19]. The overall description of this non-radiative process involves the migration of the excitation energy and a cross-relaxation mechanism in which two adjacent ions exchange energy [20].

UV-Visible Studies

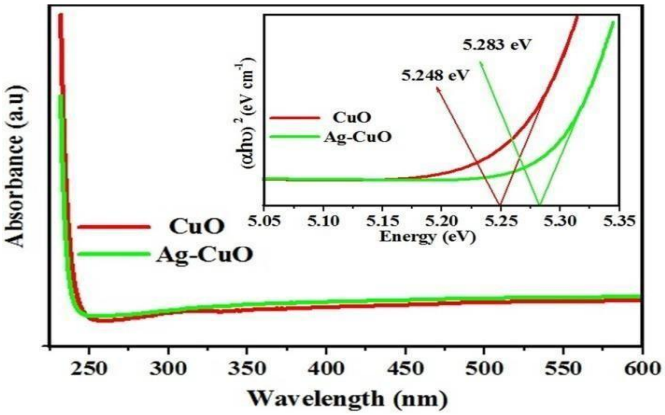

Figure 6 UV-Visible absorption spectra of CuO and Ag doped CuO nanoparticles

The absorption spectrum of the pure CuO and Ag doped CuO nanoparticles as displayed in Fig. 6. The optical properties of nanostructures strongly depend on the absorbance of the material related to the transition of charges from the valence band to the conduction band [21]. The variation in the absorption coefficient as a function of photon energy for allowed direct transitions is given by Tauc equation [2]:

$$\alpha h\upsilon = C(h - g)^n \quad \text{.....(2)}$$

where C is a constant, h is Planck's constant, υ is the frequency, and Eg is the band gap energy. The value of 1/2 is used for a semiconductor with a direct band gap. The Tauc plot is drown between $(\alpha h\upsilon)^2$ on the Y-axis and the photon energy (hυ) on the X-axis. The Tauc plot is depicted in the figure 6. From Figure 6, the band gap energy (Eg) of pure CuO nanoparticles is observed to be 5.248 eV, which increases with the doping of Ag (5.283 eV). The widening of band gap energy could be associated with the displacement of the Fermi level position into the conduction band because of the influenced rise in carrier concentration [22].

3.5 Anticancer activity

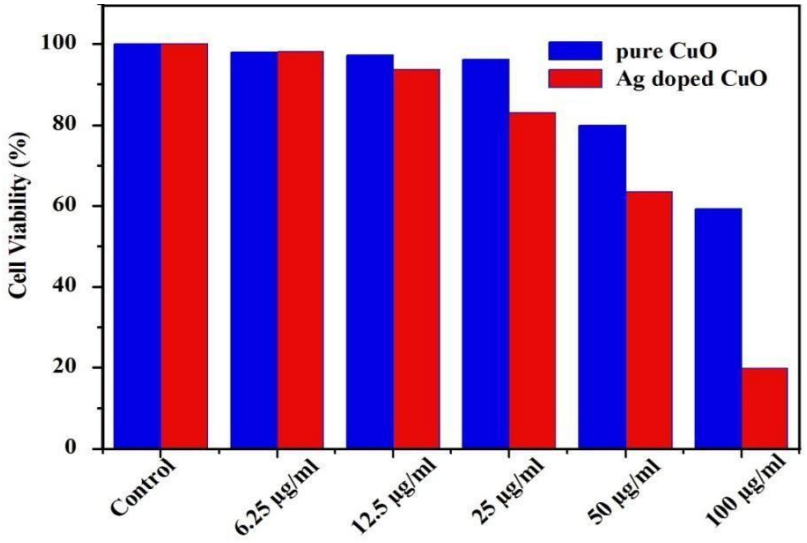

Figure 7 cell viability (%) values of AGS (Human gastric adenocarcinoma) cell lines treated by different concentrations/ doses of pure CuO and Ag doped CuO nanoparticles after the incubation period of 24hrs by MTT assay.

The pure CuO and Ag doped CuO nanoparticles were studied for their anticancer activity against AGS (Human gastric adenocarcinoma) cell using different concentration/dose of nanostructures (i.e. 6.25–100 µg/ml) by MTT assay. Figure 7 depicts the relative percent viability of the cancerous AGS cells. It has been observed that AGS cells viability is greatly inhibited by the prepared nanoparticles. Application of 100 µg/ml of the synthesized nanoparticle was resulted in better inhibition of AGS cells relative to the untreated cells. It was found that when the concentration of pure CuO was increased from 6.25 µg /ml to 100 µg /ml, the cell

viability progressively dropped from 98.03 % to 59.28 %, respectively. Nevertheless, it was possible to obtain that the cell viability gradually decreased from 98.07 % to 19.74 %, respectively, for an increase in Ag doped CuO nanoparticles concentration from 6.25 µg /ml to 100 µg /ml. Hence, these cell viability results suggest that Ag doped CuO nanoparticles possess higher anticancer activity as compared to pure CuO nanoparticles. Cytotoxicity of the CuO is generally linked with several factors such as particle size, ROS generation and release of metal ions [23,24]. Akhtar et al., [25] reported the role of the wide band gap behavior of metal-oxide nanoparticles in ROS mediated toxicity. The reduced crystallite size and wide band gap Ag doped CuO nanoparticles acting critical role in ROS mediated cytotoxicity, as evidence from XRD and UV-visible spectral analyses. The results of Ag doped CuO nanoparticles were showed that concentration/dose dependent study had reduced the cell viability of AGS - Human gastric adenocarcinoma cells lines

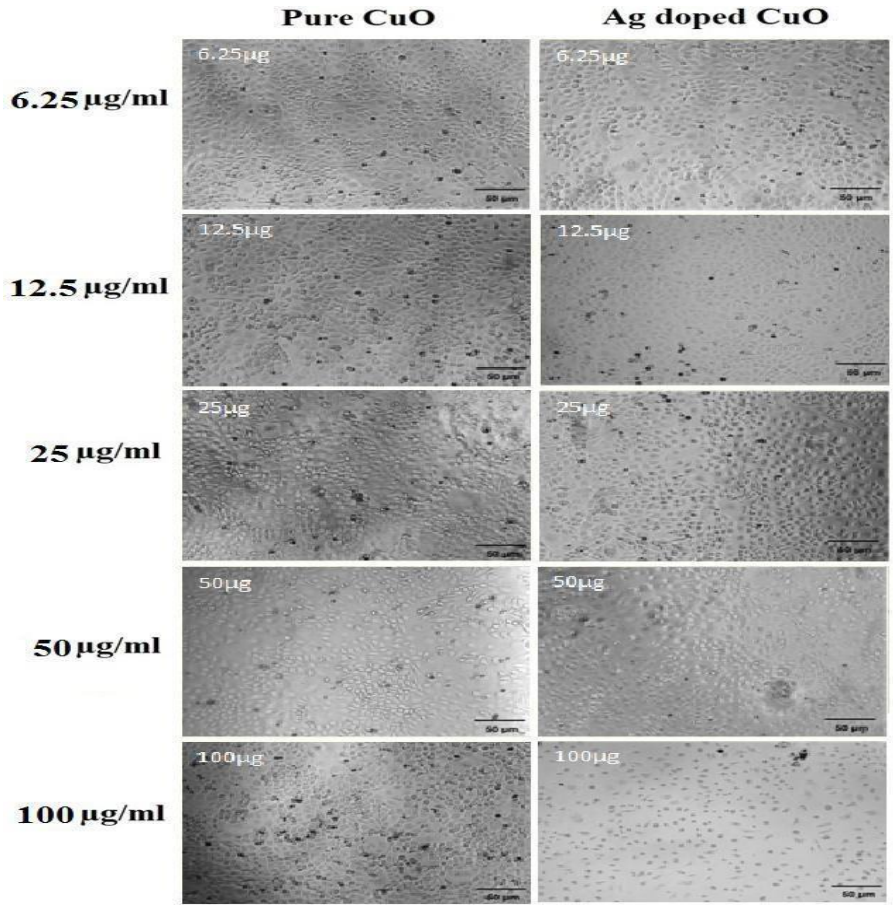

Fig. 8 Cell numbers and viability evaluated using MTT staining after 24 h seeding. (6.25 µg/ml, 12.5 µg/ml, 25 µg/ml and 50 µg/ml)

The suggested MTT test for AGS - Human gastric adenocarcinoma cells from pure CuO and Ag doped CuO nanoparticles are displayed in Fig. 8. As can be seen in the figure, the samples inhibited the growth of AGS cells using MTT staining, and as the concentrations/dose of 6.25 µg/ml, 12.5 µg/ml, 25 µg/ml, 50 µg/ml and 100 µg/ml were increased, the cell survival rates decreased in tandem. This image reveals a considerable amount of cell death after the prepared samples were treated [4]. According to the MTT results, Ag doped CuO nanoparticles had a greater probability than pure CuO as a contributor to cell death.

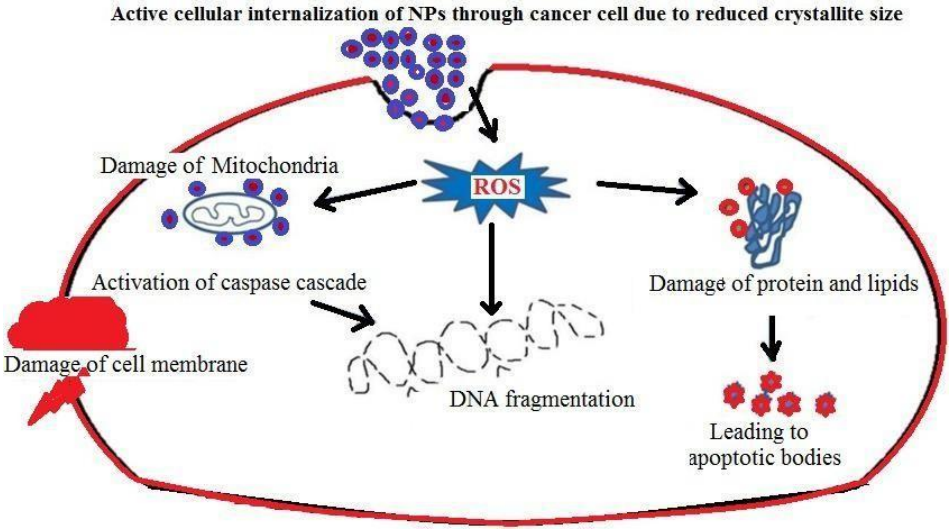

Figure 9 Mechanism involved during cytotoxicity.

The hypothetical mechanism has been described in Figure 9. The Ag doped CuO nanoparticles penetrate the cells and damages the cancer cell function [26]. The Ag doped CuO nanoparticles interact actively with negatively charged surface of cancer cell membrane, cause cell membrane breakage and destroy cancerous cells. This phenomenon follows liberation of silver and copper ions intracellular which is more effective against cytotoxicity and enzyme disruption [27]. The cytotoxic effects probably occurred due to the interference of Ag ions with the proper functioning of the protein leading to the change in the cellular chemistry also suggested by Sahin et al. [14]. This shows that Ag doped CuO nanoparticles can be a potential candidate with improved efficacy against cancerous cells. Moreover, we also perceived the superior cytotoxic influence of Cissampelos Pareira leaf extract meditated Ag doped nanoparticles than the pure ones and realized the impact of doped silver ion raising the rate of induced cytotoxicity. Therefore, the synthesis of Ag doped CuO mediated through Cissampelos

Pareira leaf extract demonstrates that these Ag doped could have chemotherapeutic effects which can be pioneered for the making of drugs.

4. Conclusion

The present study dealt with the green synthesis of CuO nanoparticles and Ag doped CuO nanoparticles employing Cissampelos Pareira leaf extract and testing their efficient as anticanceral agents against AGS human gastric adenocarcinoma cells. The crystallite size of CuO powder was determined to be 29.12 nm and that of Ag doped CuO sample was obtained to be 21.01 nm. The band gap energy of pure CuO nanoparticles is observed to be 5.248 eV, which increases with the doping of Ag (5.283 eV). According to the MTT results, Ag doped CuO nanoparticles had a greater probability than pure CuO as a contributor to cell death. Therefore, the synthesis of Ag doped CuO mediated through Cissampelos Pareira leaf extract demonstrates that these Ag doped could have chemotherapeutic effects which can be pioneered for the making of drugs.

Reference

[1] J. Samuel, J. Eugin shaji, S.D. Sahaya Jude Dhas, S. Suresh, V. Sherlin vinita, C.S. Biju, Surf. Interface Anal. 55 (2023) 307–320.

[2] M.M.S. Al Mazroui, G. Devi, A.M.A.H. Al Abdali, S.M.K. Al Alawi, BIO Web Conf. 160 (2025).

[3] A. Muthuvel, M. Jothibas, C. Manoharan, S.J. Jayakumar, Res. Chem. Intermed. 46 (2020) 2705–2729.

[4] A. Muthuvel, M. Jothibas, C. Manoharan, Nanotechnol. Environ. Eng. 5 (2020).

[5] P.S.V. Sandhya, S.R. Kunjikannan, J. Environ. Heal. Sci. Eng. (2023).

[6] S. Vasantharaj, S. Sathiyavimal, P. Senthilkumar, F. LewisOscar, A. Pugazhendhi, J. Photochem. Photobiol. B Biol. 192 (2019) 74–82.

[7] H.N. Cuong, S. Pansambal, S. Ghotekar, R. Oza, N.T. Thanh Hai, N.M. Viet, V.H. Nguyen, Environ. Res. 203 (2022) 111858.

[8] S. Kumari, Anmol, V. Bhatt, P.S. Suresh, U. Sharma, J. Ethnopharmacol. 274 (2021).

[9] G. Amresh, P.N. Singh, C.V. Rao, J. Ethnopharmacol. 116 (2008) 454–460.

[10] G. Amresh, P.N. Singh, C. V. Rao, J. Ethnopharmacol. 111 (2007) 531–536.

[11] D. Reshmi Agnes Preethi, S. Prabhu, V. Ravikumar, A. Philominal, Mater. Today Commun. 33 (2022) 104462.

[12] V.V.T. Padil, M. Černík, Int. J. Nanomedicine 8 (2013) 889–898.

[13] G. Ren, D. Hu, E.W.C. Cheng, M.A.

Vargas-Reus, P. Reip, R.P. Allaker, Int. J. Antimicrob. Agents 33 (2009) 587–590.

[14] C. Sahin, U. Arabaci, D.T. Bulut, P. Obakan Yerlikaya, J. Inorg. Organomet. Polym. Mater. (2025).

[15] M. Zahoor, A. Arshad, Y. Khan, M. Iqbal, S.Z. Bajwa, R.A. Soomro, I. Ahmad, F.K. Butt, M.Z. Iqbal, A. Wu, W.S. Khan, Appl. Nanosci. 8 (2018) 1091–1099.

[16] Y. Li, W. Yin, R. Deng, R. Chen, J. Chen, Q. Yan, B. Yao, H. Sun, S.H. Wei, T. Wu, NPG Asia Mater. 2012 411 4 (2012) e30–e30.

[17] Z.H.C. and G.Z.Y. L Z Cao, B L Cheng, S Y Wang, W Y Fu, S Ding, Z H Sun, H T Yuan, Y L Zhou, J. Phys. D. Appl. Phys. 39(13) (2006) 2819.

[18] H.W. Seo, S.Y. Bae, J. Park, H. Yang, K.S. Park, S. Kim, J. Chem. Phys. 116 (2002) 9492–9499.

[19] S. Chen, X. Zhao, H. Xie, J. Liu, L. Duan, X. Ba, J. Zhao, Appl. Surf. Sci. 258 (2012) 3255–3259.

[20] H. Rinnert, P. Miska, M. Vergnat, G. Schmerber, S. Colis, A. Dinia, D. Muller, G. Ferblantier, A. Slaoui, Appl. Phys. Lett. 100 (2012) 1–4.

[21] S. Shabna, J.E. Shaji, S.S.J. Dhas, S. Suresh, A. Aravind, S.A. Thomas, V.S. Vinita, J. Samuel, C.S. Biju, J. Clust. Sci. (2023) 1–10.

[22] J. Samuel, S. Suresh, S. Shabna, V. Sherlin Vinita, N. Joslin Ananth, P.M. Shajin Shinu, A. Mariappan, T. simon, Y. Samson, C.S. Biju, Phys. E Low-Dimensional Syst. Nanostructures 143 (2022) 115374.

[23] A.K. Chitoria, A. Mir, M.A. Shah, Ceram. Int. 49 (2023) 32343–32358.

[24] P.C. Nagajyothi, M. Pandurangan, M. Veerappan, D.H. Kim, T.V.M. Sreekanth, J. Shim, Mater. Lett. 216 (2018) 58–62.

[25] M.J. Akhtar, S. Kumar, H.A. Alhadlaq, S.A. Alrokayan, K.M. Abu-Salah, M. Ahamed, Toxicol. Ind. Health 32 (2016) 809–821.

[26] G.K. Prashanth, H.M. Sathyananda, P.A. Prashanth, M. Gadewar, M. Mutthuraju, S.R.B. Prabhu, B.M. Nagabhushana, C. Shivakumara, S. Rao, D. Mohanty, Appl. Phys. A Mater. Sci. Process. 128 (2022).

[27] S.U. R, M.A. Alnuwaiser, L.M. S, V.S. Betageri, S. V. A, M.I. Khan, K. Guedri, J. Indian Chem. Soc. 99 (2022).